

Regulation of immune responses to therapeutic factor VIII by transplacental delivery of Fc-fused immunodominant factor VIII domains or peptides

Alejandra Reyes-Ruiz,¹ Sandrine Delignat,¹ Aurélien Azam,¹ Victoria Daventure,¹ Leslie Dourthe,¹ Angelina Mimoun,¹ Geneviève McCluskey,² Maria T. Georgescu,³ David Lillicrap,³ Jordan D. Dimitrov¹ and Sebastien Lacroix-Desmazes¹

¹Institut National de la Santé et de la Recherche Médicale, Centre de Recherche des Cordeliers, CNRS, Sorbonne Université, Université Paris Cité, Paris, France; ²Laboratory for Hemostasis, Inflammation & Thrombosis, Unité Mixte de Recherche 1176, Institut National de la Santé et de la Recherche Médicale, Université Paris-Saclay, Le Kremlin-Bicêtre, France and ³Department of Pathology and Molecular Medicine, Queen's University, Kingston, Ontario, Canada

Correspondence: S. Lacroix-Desmazes
sebastien.lacroix-desmazes@inserm.fr

Received: November 27, 2024.
Accepted: March 3, 2025.
Early view: March 13, 2025.

<https://doi.org/10.3324/haematol.2024.287057>

©2025 Ferrata Storti Foundation

Published under a CC BY-NC license



Supporting information

Supplemental Materials and Methods

Sources of Fc-fused FVIII variants. The mutants rFVIII^{C1C2}Fc bearing the R2090A, K2092A, F2093A, R2215A mutations and rFVIII^{N2118Q}Fc were generated using site-directed mutagenesis with the In-Fusion system (Takara Bio, Shiga, Japan). Templates of cDNA encoding human B domain-deleted (BDD) FVIII (with the 14-amino-acid-long segment SFSQNPPVLKRHQR in place of the B domain), and the cDNA encoding a human Fc γ 1 domain dimerized with a linker (provided by Sanofi)¹ were used. The sequences were cloned in the ReNeo plasmid and validated by standard sequencing analysis. BHK-M cells were transfected and the clones resistant to neomycin were selected using Geneticin-sulfate (500 μ g/ml, Sigma-Aldrich, St. Louis, MO). FVIII-producing clones were screened with a FVIII chromogenic assay (Siemens Healthcare, Erlangen, Germany). Clones with the highest expression for each rFVIII Fc mutant were selected and scaled up to near confluency before switching the medium to serum free AIM-V medium (Thermo Scientific). Medium was collected every 24 hrs. Purification of Fc fused FVIII molecules was performed by affinity chromatography on VIIIselect column (GE Healthcare, Chicago, IL), followed by anion-exchange chromatography on HiTrap Resource Q column (GE Healthcare).²

Sources of Fc-fused FVIII domains. The Fc-fused FVIII activated LCh (domains A3C1C2) was purified from rFVIII Fc (Eloctate®, 4000 IU) by size exclusion chromatography on a superdex 200 Hiload 26/600 column after digestion by thrombin (250 IU, Sigma Aldrich). Eluted fractions were concentrated using Amicon system and validated by SDS-PAGE and ELISA. The cDNA encoding codon-optimized human

FVIII was amplified and fused to the cDNA encoding a dimerized Fc-linker-Fc (provided by Sanofi) prior to insertion in the pALL expression vector with In-Fusion cloning kits (Takara). Appropriate primers were designed to clone the A1a1, A2a1, a3A3C1, C1 and C2 FVIII domains. To increase the levels of production, the F309S mutation was introduced in the A1 domain.³ To abrogate the binding to FcγRs⁴ or to FcRn,⁵ the mutations N297A (**supplemental Fig. S1A**) or I253A/H310A/H435A (IHH) (**supplemental Fig. S1C**) were introduced in the Fc sequence of C2Fc by site-directed mutagenesis using In-Fusion system. Expi293 cells were transiently transfected with the different constructs using the Expi293 expression system (Thermo Scientific). After 3-6 days of culture in serum free conditions, supernatants were collected, and Fc-fused proteins were detected by ELISA and Western blot. When amounts were sufficient, the Fc-fused domains were purified by affinity chromatography (HiTrap rProteinA FF, GE Healthcare), further dialyzed against PBS and expected molecular weights validated by SDS-PAGE (**supplemental Fig S6A**).

Sources of FVIII-derived immunodominant peptides fused with Fc (iPep-FVIII-Fc).

The cDNA encoding the FVIII-derived immunodominant peptides⁶ (**supplemental Table S3**) as well as the linker sequences, referenced as XTEN blocks⁷ inserted between the peptides (**supplemental Table S4**), were obtained from GeneArt (Thermo Scientific). The sequences were amplified and fused to the cDNA encoding a dimerized Fc-linker-Fc (provided by Sanofi) prior to insertion in the pALL expression vector with In-Fusion cloning kit (Takara). Appropriate primers were designed to clone the Peptide 1-2-3Fc and Peptide 4-5-6-7Fc (**Fig 5C**). Expi293 cells were transiently transfected with the different constructs using Expifectamine kit (Thermo Scientific). After 6 days of culture in serum free conditions, supernatants were collected, and the

iPep-FVIII^h were detected by ELISA. The molecules were purified by affinity chromatography (HiTrap rProteinA FF, GE Healthcare), further dialyzed against PBS and validated by SDS-PAGE (**supplemental Fig S6B**).

ELISA for the detection of molecules in mouse plasma. In the case of rFVIII^h and rFVIII^h mutants, ELISA plates (Thermo Scientific) were coated with GMA-8015 (anti-A2 domain, Green Mountain, Burlington, VT) and GMA-8026 (anti-C2 domain, Green Mountain) at 1 µg/ml in PBS overnight at 4°C. After the addition of plasma, bound FVIII was revealed using a biotinylated sheep polyclonal anti-FVIII antibody (SAF8C, Stago, Asnières-sur-Seine, France), followed by streptavidin coupled to horseradish peroxidase (HRP). For other Fc-fused molecules, ELISA plates were coated with a mouse anti-human IgG Fc (LS-C69574, LSBio, Seattle, WA) at 5 µg/ml and revealed using an anti-human IgG Fc conjugated to HRP (9040-05, Southern Biotech). In addition, C2Fc and C2Fc mutants were quantified by coating the ELISA plates with anti-human FVIII-C2 domain (GMA-8026) at 2 µg/ml and revealed using an anti-human Ig Fc conjugated to HRP (2047-05, Southern Biotech). For all the quantifications of proteins in plasma by ELISA, wells were blocked with 20 mM HEPES, 0.154M NaCl and 5% BSA. Plasma samples were then diluted in 20mM HEPES, 0.4 M NaCl, 0.1% tween 20 and incubated in the coated wells for 1hr at 37°C. Plates were revealed using TMB and absorbance was read at 450 nm. Of note, each molecule was measured in the plasma of mice using a standard curve generated with the corresponding purified molecule.

Activated partial thromboplastin time (aPTT). An aPTT assay was performed to quantify the activity of FVIII in fetuses' plasma. The samples were diluted 1/24 in

STA®-ImmunoDef VIII (Stago) and 25 µl of aPTT-reagent (Stago) were added to 50µl of the diluted samples. The clotting reaction was initiated by adding 25µl of CaCl₂ (Stago), and the time was quantified using a Diagnostica Stago-ST4 coagulation analyzer. The concentration of activated FVIII was obtained using a standard curve of rFVIII Fc (Eloctate®), and activities were calculated considering a specific activity of 4265 IU/mg.

Induction of tolerance experiments. Pregnant Hemophilia A (HA) mice were injected intravenously (iv) with 227 pmoles of rFVIII Fc or 1500 pmoles for the other molecules at E16, E17 and E18. The immune response to therapeutic BDD-FVIII was investigated in offspring at 4-6 weeks of age by following the development of total and neutralizing anti-FVIII IgG upon weekly challenge with 1 µg BDD-FVIII per mice. Different sources of BDD-FVIII were used depending on availability: Novoeight (Novo Nordisk A/S) or Nuwiq (Octapharma). Neutralizing anti-FVIII IgG were measured using a functional coagulation assay (Bethesda assay) as previously described² and levels of anti-FVIII IgG by ELISA. Full-length FVIII (Advate, Takeda) was coated on ELISA plates at 2 µg/mL at 4°C overnight. After the addition of mice sera, the presence of anti-FVIII IgG was detected using a goat anti-mouse IgG conjugated with HRP (1030-05, Southern Biotech, Birmingham, AL). A pool of mouse anti-FVIII monoclonal antibodies (mAbs) including an anti-a1 (ESH-5, Invitech Ltd, Huntingdon, United Kingdom) and anti-A2 (GMA-8015, Green Mountain), and anti-C2 (ESH-8, Invitech Ltd) were used as standards. Plates were revealed using o-phenylenediamine dihydrochloride (OPD) and absorbance was read at 492 nm. Anti-FVIII IgG titers are depicted in µg/ml-equivalent to the pool of mouse anti-FVIII mAbs.

Microscopy assays. The human choriocarcinoma cell line BeWo (CCL98, American Type Culture Collection, MD, USA) was cultured in Ham's F-12K medium (Thermo Scientific) supplemented with 10% fetal calf serum (FCS) and 1% penicillin–streptomycin (complete Ham's F-12K), and routinely grown in plastic tissue-culture dishes. BeWo cells (2×10^5 cells per well) were plated in 24-well plates with a poly-L-lysine (Sigma-Aldrich) pre-coated coverslip in complete Ham's F-12K. After 48hr, cells were rinsed with PBS+CaCl₂+MgCl₂ (Thermo Scientific) and pre-pulsed with 100 µg/mL Alexa 555-labelled dextran (D34679, Thermo Scientific) for 2 hrs for lysosomal staining. Cells were washed and pulsed with 114 nM rFVIII^{HH}Fc (Eloctate®), or C2Fc or C2Fc^{HH} at 37°C for 30 min in 0.5% FCS-PBS+CaCl₂+MgCl₂. For endocytosis experiments, cells were immediately fixed, while for lysosomal co-staining evaluation, cells were washed with PBS+CaCl₂+MgCl₂ (Thermo Scientific) followed by a chase of 6 hrs in complete media. After fixation, cells were permeabilized with 0.2% PBS-Triton for 10 min and incubated with 1% PBS- BSA for 35 min. Detection of early endosomes was performed using 2 µg/mL rabbit anti-EEA1 (ab2900, Abcam, Cambridge, UK) incubated for 2 hrs followed by 2 hrs incubation with goat anti-rabbit Alexa Fluor 488. Fc-fused molecules were stained with 10 µg/mL goat anti-human IgG Alexa Fluor 647 (A-21445, Thermo Scientific) for 2 hrs. After staining, cells were washed, and nuclei were counterstained in blue with Hoechst 33342 dye (H3570, Thermo Scientific). Cells were washed again, and the coverslips were mounted in slides using ProLong Gold antifade reagent (P36930, Thermo Scientific). Images were acquired with the ZEISS LSM 710 Confocal Microscope (Zeiss, Oberkochen, Germany).

Evaluation of surface electrostatic potentials. The 3D structures of human BDD-FVIII (6MF2), human anti-HIV m66.6 Fab (4NRZ), human anti-HIV VRC01-class DRVIA7 Fab (5CD5) were obtained from the PDB database (<https://www.rcsb.org/>).⁸ The Iterative Threading Assembly Refinement (I-TASSER) web server (<https://zhanglab.dcmf.med.umich.edu/I-TASSER/>) was used to modelized the FVIII^{C1C2} mutant. Quality assessment of the model was performed using the SAVES platform (<https://saves.mbi.ucla.edu/>), and their Ramachandran plot distributions were evaluated through the PDBsum server (<https://www.ebi.ac.uk/thornton-srv/databases/cgi-in/pdbsum/>).⁹ Energy minimization of the model was done using the SWISS-PDB Viewer tool (<https://www.expasy.org/spdbv>) to alleviate internal constraints and reduce the overall potential energy.¹⁰ The surface electrostatic potentials of the proteins and of the modelized BDD-FVIII^{C1C2} mutant were calculated by the Poisson-Boltzmann computational method using SWISS-PDB viewer.

FcRn binding by surface plasmon resonance. Binding to the human and mouse FcRn of the Fc-fused proteins was evaluated by surface plasmon resonance using a Biacore 2000 (Cytiva, Marlborough, MA). Biotinylated hFcRn or mFcRn (kindly given by Dr Sune Justesen, Immunitrack, Danemark) were diluted in tris-citrate buffer (100 mM Tris, 100 mM NaCl, 5% glycerol and 0.1% tween 20 at pH 6) and immobilized on a streptavidin-coated sensor chip at a protein surface density of approximately 0.5 ng/mm² (450–550 RU). The Fc-fused proteins were injected at 25°C after being diluted in running buffer (100 mM Tris, 100 mM NaCl, 5% glycerol and 0.1% tween 20, pH 6). Injections were performed using the KINJECT mode (flow, 30 µl/min; volume, 120 µl; dissociation time, 300 s). To regenerate, 15 µl of 100 mM Tris, 100 mM NaCl pH 7.8 was injected. The binding constants at pH 6 were evaluated in 2-fold serial

dilutions of the samples (25 to 0.097 nM) and calculated from the sensorgrams using the 1:1 Langmuir or binding with drifting baseline model of BIAevaluation software. The quality of the fitting of the models was judged by the low values of the χ^2 , not exceeding the 10% of the highest RU. Equilibrium dissociation constants were calculated from the values of association and dissociation rate constants, as $K_D = K_d/K_a$.

Binding to FcγRs. Fc-fused proteins were incubated at 10 nM with human FcγRIII transfected BW5147 thymoma (provided by Dr Philipp Kolb, Institute of Virology, University Medical Center, Freiburg, Germany)¹¹ in RPMI-1640, 0.5% fetal calf serum, 100 U/mL penicillin, 100 mg/mL streptomycin. After 90 min of incubation at 4°C, cells were washed with ice cold PBS and bound Fc-fused proteins were detected with a PE conjugated goat anti-human Fc (Thermo Scientific). FACS analysis was performed on live cells using fixable viability dye eFluor780 (Thermo Scientific) staining. Data was acquired using the BD LSRII and analyzed on the FACS Diva software (Becton Dickinson, Franklin Lakes, New Jersey, USA).

Binding to VWF. ELISA plates (Thermo Scientific) were coated overnight at 4°C with 2 µg/mL VWF (Wilfactin, LFB, France). The Fc-fused FVIII variants were diluted in PBS-1% milk, 0.1% tween 20 and added to the plates. Bound molecules were detected with a biotinylated mouse monoclonal anti-FVIII A2 domain IgG (GMA8015, Green Mountain), streptavidin conjugated to HRP (R&D Systems) and TMB substrate. Optical densities were measured at 450 nm with a TECAN Infinite 200.

References

1. Peters RT, Toby G, Lu Q, et al. Biochemical and functional characterization of a recombinant monomeric factor VIII–Fc fusion protein. *Journal of Thrombosis and Haemostasis* 2013;11(1):132–141.
2. Delignat S, Rayes J, Dasgupta S, et al. Removal of Mannose-Ending Glycan at Asn2118 Abrogates FVIII Presentation by Human Monocyte-Derived Dendritic Cells. *Front Immunol* 2020;11393.
3. Poonthong J, Pottekat A, Siirin M, et al. Factor VIII exhibits chaperone-dependent and glucose-regulated reversible amyloid formation in the endoplasmic reticulum. *Blood Reviews* 2020;13513.
4. Sazinsky SL, Ott RG, Silver NW, Tidor B, Ravetch JV, Wittrup KD. Aglycosylated immunoglobulin G₁ variants productively engage activating Fc receptors. *Proc Natl Acad Sci USA* 2008;105(51):20167–20172.
5. Medesan C, Matesoi D, Radu C, Ghetie V, Ward ES. Delineation of the amino acid residues involved in transcytosis and catabolism of mouse IgG1. *J Immunol* 1997;158(5):2211–2217.
6. Steinitz KN, Van Helden PM, Binder B, et al. CD4+ T-cell epitopes associated with antibody responses after intravenously and subcutaneously applied human FVIII in humanized hemophilic E17 HLA-DRB1*1501 mice. *Blood* 2012;119(17):4073–4082.
7. Schellenberger V, Wang C, Geething NC, et al. A recombinant polypeptide extends the in vivo half-life of peptides and proteins in a tunable manner. *Nat Biotechnol* 2009;27(12):1186–1190.
8. Berman HM, Westbrook J, Feng Z, et al. The Protein Data Bank. *Nucleic Acids Res* 2000;28(1):235–242.
9. Laskowski RA, Jabłońska J, Pravda L, Vařeková RS, Thornton JM. PDBsum: Structural summaries of PDB entries. *Protein Sci* 2018;27(1):129–134.
10. Bhale AS, Venkataraman K. Delineating the impact of pathogenic mutations on the conformational dynamics of HDL's vital protein ApoA1: a combined computational and molecular dynamic simulation approach. *J Biomol Struct Dyn* 2023;41(24):15661–15681.
11. Lagassé HAD, Hengel H, Golding B, Sauna ZE. Fc-Fusion Drugs Have FcγR/C1q Binding and Signaling Properties That May Affect Their Immunogenicity. *AAPS J* 2019;21(4):62.

Supplemental Tables

Table S1. Kinetic parameters of the binding of Fc-fused molecules to mouse FcRn (mFcRn) at pH 6.

	k_{on} ($\text{M}^{-1} \cdot \text{s}^{-1}$)	k_{off} (s^{-1})	K_{D} (nM)	Chi^2
rFVIII_{FC}	0.96×10^6	2.78×10^{-4}	0.29	12
rFVIII_{FC}^{N297A}	0.90×10^6	5.63×10^{-4}	0.62	3.3
rFVIII^{C1C2}_{FC}	0.48×10^6	7.28×10^{-4}	1.51	7
rFVIII^{N2118Q}_{FC}	1.09×10^6	3.87×10^{-4}	0.36	2
C2_{FC}	1.45×10^6	4.33×10^{-4}	0.30	16
C2_{FC}^{N297A}	1.83×10^6	5.94×10^{-4}	0.33	3
rFIX_{FC}	1.45×10^6	6.22×10^{-4}	0.43	2.4
VRC01	0.62×10^6	6.44×10^{-4}	1.03	6
m66.6	0.90×10^6	2.0×10^{-4}	0.22	12

Table S2. Kinetic parameters of the binding of Fc-fused molecules to human FcRn (hFcRn) at pH 6.

	$k_{on} (M^{-1}.s^{-1})$	$k_{off} (s^{-1})$	$K_D (nM)$	χ^2
rFVIII_{FC}	2.14×10^6	3.05×10^{-3}	1.40	9
rFVIII_{FC}^{N297A}	2.70×10^6	3.68×10^{-3}	1.36	0.6
rFVIII^{C1C2}_{FC}	8.12×10^5	3.48×10^{-3}	4.29	3.4
rFVIII^{N2118Q}_{FC}	1.16×10^6	3.02×10^{-3}	2.61	2.7
C2_{FC}	2.62×10^6	2.47×10^{-3}	0.94	0.5
C2_{FC}^{N297A}	2.80×10^6	2.99×10^{-3}	1.07	0.34
rFIX_{FC}	1.10×10^6	2.46×10^{-3}	2.30	6
VRC01	1.36×10^6	6.56×10^{-3}	4.82	1.79
m66.6	1.50×10^6	2.80×10^{-3}	1.86	14

Table S3. Immunodominant FVIII-derived peptide sequences

Peptide	Domain	Sequence (Amino Acids)
P1	A3	AAVERLWDYGMSSSPHVLRNRAQSGS
P2	A2	SDPRCLTRYYSFVNMERDLA
P3	A1	RPPWMGLLGPTIQAE
P4	A1	LPVDARFPFPRVPKSFNFNTS
P5	C1	IKHNIFNPPIIARYIRLH
P6	C1	TKEPFSWIKVDLLAPMIIHGIKTQGARKKFS
P7	C2	YFTNMFATWSPSKARLHL

Table S4. XTEN block sequences

XTEN BLOCK	Sequence (Amino Acids)
B1	GTSESATPESGPG
B2	SEPATSGSETP
B3	STEPSEGSAPG

Supplemental Figures

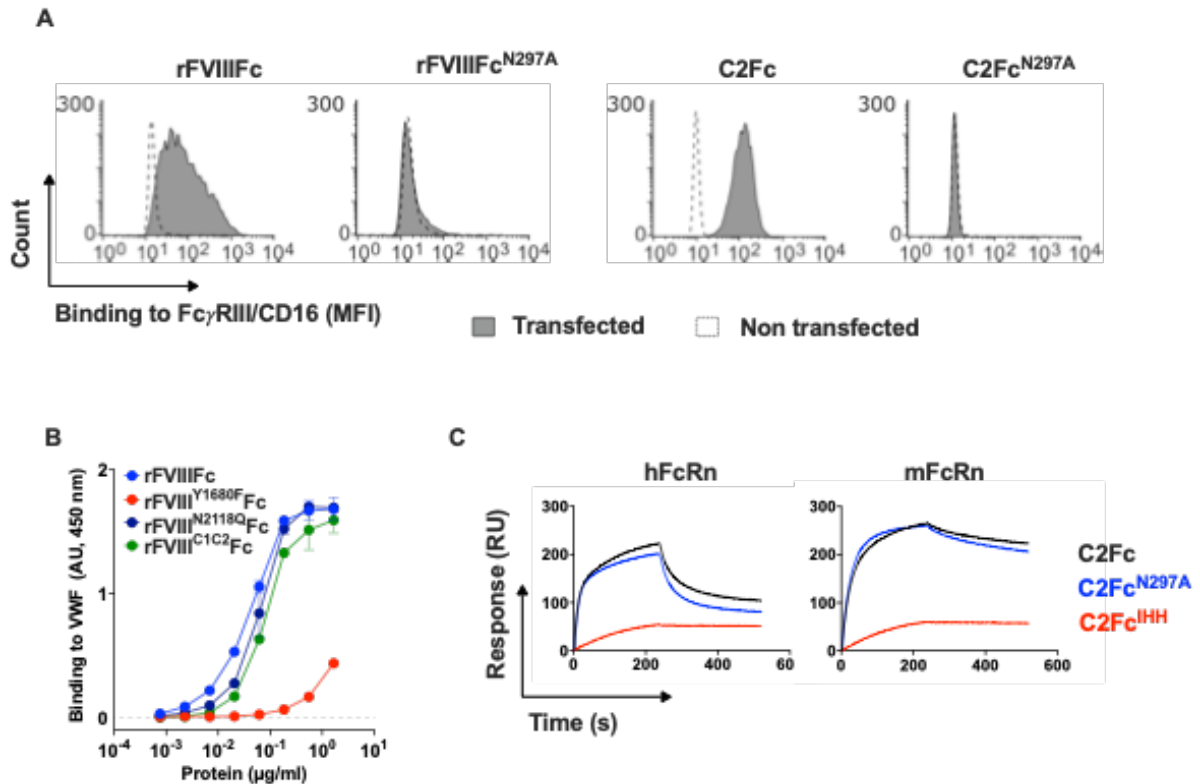


Figure S1. Characterization of rFVIII Fc and C2Fc variants. **A.** Representative FACS histograms of the binding of rFVIII Fc, rFVIII Fc^{N297A}, C2Fc or C2Fc^{N297A} to BW5147 thymoma cells no transfected (dotted) or stably transfected to express the human CD16 (Fc_γRIIIa, grey). **B.** Binding of rFVIII Fc (blue), rFVIII^{Y1680F} Fc (red), rFVIII^{N2118Q} Fc (dark blue), rFVIII^{C1C2} Fc (green) to VWF by ELISA. Fc-fused FVIII molecules were incubated in serial dilutions on plates coated with human plasma-derived VWF and detected using a biotinylated mouse monoclonal anti-FVIII A2 domain IgG. Binding is expressed as arbitrary units (AU) as mean±SD (triplicates) based on the optical density measured at 450 nm. The graph is representative of two independent experiments. **C.** Real time interaction profiles of C2Fc (black line), C2Fc^{N297A} (blue line) and C2Fc^{IHH} (red line) with immobilized human or murine FcRn at pH 6.

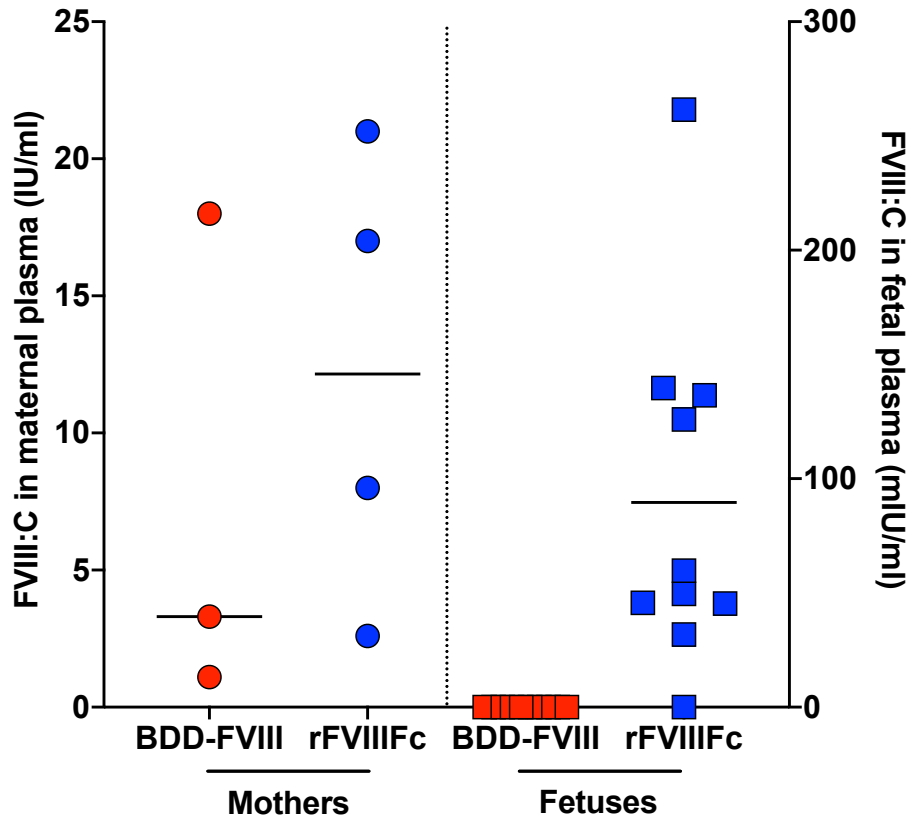


Figure S2. FVIII activity in plasma from pregnant Hemophilia A (HA) mice and their fetuses following injection of FVIII or rFVIII Fc. E19 pregnant HA mice were injected iv with BDD-FVIII (376 IU) or rFVIII Fc (376 IU). Plasma was collected 3 hrs later. FVIII activity was measure using a functional coagulation chromogenic assay and is expressed in IU/ml in maternal plasma, and in mIU/ml in fetal plasma. In the case of pregnant mice, each dot represents results from a single mother. In the case of fetuses, each dot represents a pool of plasma from 2 to 3 fetuses.

Figure S3

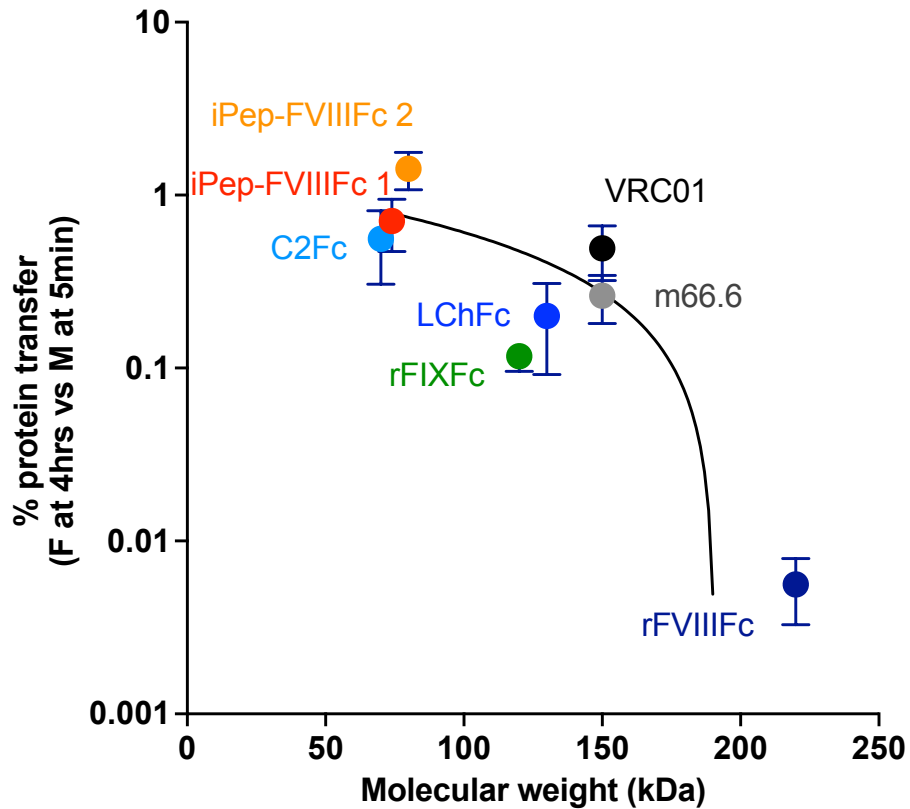


Figure S3. Correlation between size of molecules and their % protein transfer. The % protein transfer is depicted as the percentage of antigen detected in the fetuses' plasma at 4 hrs versus that detected in mothers' plasma at 5 min. The % protein transfer (mean \pm SD) was plotted as a function of the molecular weight of the molecules: C2Fc (70 kDa), iPep-FVIII Fc 1 (74 kDa), iPep-FVIII Fc 2 (80 kDa), rFIXFc (120 kDa), m66.6 (150 kDa), VRC01 (150 kDa), rFVIII Fc (220 kDa), LChFc (130 kDa). Experimental data were fitted by simple linear regression (slope: -0,007; R^2 : 0.399; $P=0.0001$). VRC01 and m66.6 are monoclonal human IgG1. iPep-FVIII Fc 1 and 2 are FVIII peptides fused to human Fc γ 1 (see **supplemental Tables S3** and **S4**, and **Fig 5C**). LChFc is the light chain of FVIII purified from activated rFVIII Fc.

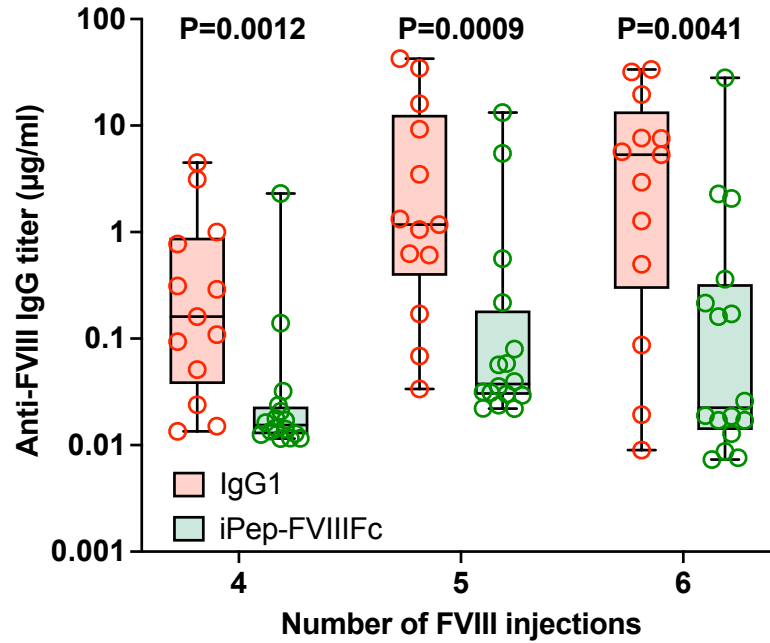


Figure S4: Reduction of the immune response towards FVIII in progeny from mothers injected with Fc-fused FVIII-derived immunodominant peptides during pregnancy. The humanized monoclonal IgG1, trastuzumab (1500 pmoles, Herceptin®) or a pool of iPep-FVIII Fc 1 and 2 (1500 pmoles each) were injected iv into pregnant Hemophilia A mice at E16, E17 and E18. The 4-week-old progeny was injected weekly with BDD-FVIII (1 µg/mouse). After 4, 5 and 6 injections, blood was collected, anti-FVIII IgG titers were quantified by ELISA (expressed in µg/ml units and depicted as boxes and whiskers with minimal and maximal values). Empty circles represent individual animals. Statistical significances were assessed at each time point using the two-sided non-parametric Mann-Whitney test.

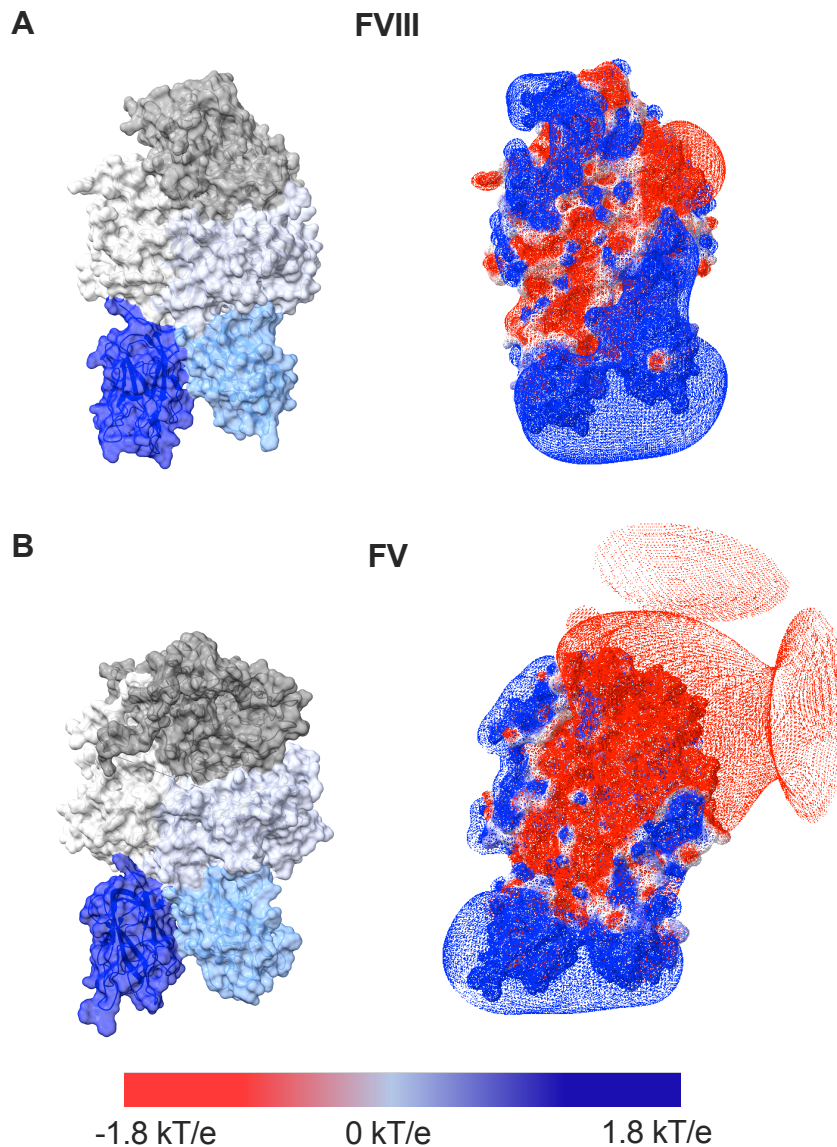


Figure S5. Surface electrostatic potential of FV. The figure depicts the structures of human B domain-deleted FVIII (PDB: 6MF2, panel A), human B domain-deleted factor V (PDB: 7KVE, panel B). The FVIII and FV A1, A2, A3, C1 and C2 domains are depicted in white, gray, light blue, cyan and cobalt blue, respectively. Electrostatic potential maps calculated using the Poisson-Boltzmann method (SWISS-PDB viewer) are shown on the left. Negative potentials are depicted in red and positive potentials in blue.

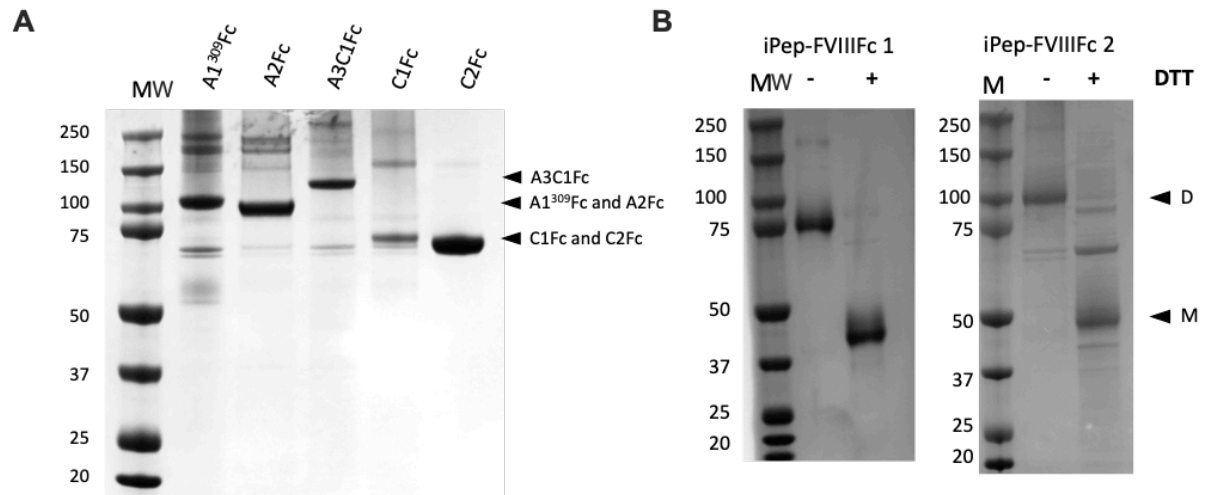


Figure S6. SDS-PAGE of A1Fc, A2Fc, A3C1Fc, C1Fc and C2Fc (**A**). SDS-PAGE of iPep-FVIII Fc 1 and 2 in presence (+) or absence (-) of DTT (**B**). MW: molecular weight markers; D: dimers; M: monomers.